frontiers | Frontiers in Materials

ORIGINAL RESEARCH
published: 13 May 2022
doi: 10.3389/fmats.2022.894451

AgNP-AC Composite Fibers and its Adsorption and Antibacterial Properties

Dandan Liu[1,2], *Chuanwei Zhang*[2]*, *Bin Wang*[1], *Wenwen Quan*[2] *and Chao Xu*[2]*

[1]*Department of Mechanical and Aerospace Engineering, Brunel University London, Uxbridge, United Kingdom,* [2]*College of Mechanical Engineering, Xi'an University of Science and Technology, Xi'an, China*

In this study, the electrospinning method was used to prepare silver nanoparticle–activated carbon (AgNP-AC) composite nanofiber membranes, aiming to obtain a high-performance dual-functional filter composite fiber membrane with good antibacterial and adsorption properties. A scanning electron microscope (SEM), X-ray diffractometer (XRD), and other instruments were used to characterize the morphology and structure of the composite nanofibers. The effects of different concentrations of activated carbon, silver, and polymer (polyethylene–vinyl alcohol—EVOH) on the fiber morphology were discussed. The adsorption performance and antibacterial performance of the composite fiber membrane were investigated to verify the mutual influence of silver and activated carbon. The results show that with the increase in the activated carbon and silver concentration, the fiber diameter of the AgNP-AC membrane increase and the diameter distribution tends to become uniform. When the mass fraction of polymer EVOH is 10% and the concentration ratio of silver nitrate and carbon is 0.05 and 0.085 (g/ml), the adsorption performance of the composite fiber membrane is at the best with an adsorption rate of 94.07%. The AgNP-AC composite nanofiber membrane also demonstrates a good antibacterial function against *Staphylococcus aureus* and is most effective in the first 8 h. However, it is found that the silver concentration is proportional to the antibacterial ability, but the activated carbon has a certain inhibitory effect on the antibacterial properties.

Keywords: electrospinning, nanofiber, adsorptive property, antimicrobial property, functional materials

OPEN ACCESS

Edited by:
Wenbo Wang,
Inner Mongolia University, China

Reviewed by:
Dawei Gao,
Yanshan University, China
Hossam Elsayed Emam,
National Research Centre, Egypt

***Correspondence:**
Chuanwei Zhang
zhangcw@xust.edu.cn
Chao Xu
Chaoxu@xust.edu.cn

Specialty section:
This article was submitted to Polymeric and Composite Materials, a section of the journal Frontiers in Materials

Received: *11 March 2022*
Accepted: *11 April 2022*
Published: *13 May 2022*

Citation:
Liu D, Zhang C, Wang B, Quan W and Xu C (2022) AgNP-AC Composite Fibers and its Adsorption and Antibacterial Properties. Front. Mater. 9:894451. doi: 10.3389/fmats.2022.894451

INTRODUCTION

Air pollution has become a major problem affecting human health, with evidence showing that airborne fine particulate pollutants of less than 2.5 μm (i.e., PM2.5) are linked to poor health (Chen et al., 2019; Qiu et al., 2015). Currently, two approaches have been commonly adopted to address the problem: one is to reduce the emission of pollutants and the other one is to remove the pollutants by using filter membrane materials for a local and confined space (Gao et al., 2019). For the latter one, traditional filter materials are mainly composed of micron fibers, such as melt-blown fibers, aramid, and glass fibers (Matulevicius et al., 2016; Liu et al., 2019; Tian et al., 2018). However, these traditional fiber materials generally are only suitable for micron-level particles.

Recent studies show that nanofiber membranes fabricated by the electrospinning technology have advantageous potential for applications in preventing submicron-level air pollution, due to the membranes" high void ratios, large specific surface areas, and small fiber diameters (Khandaker et al.,

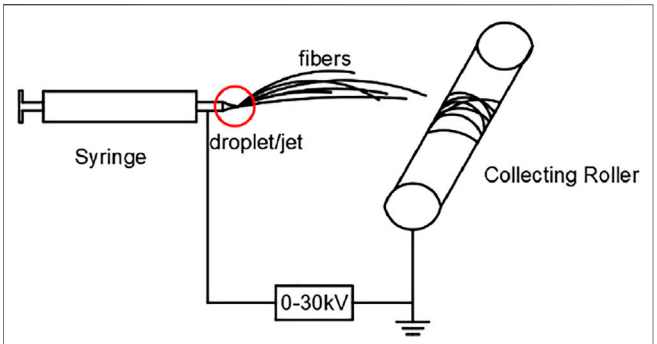

FIGURE 1 | Schematic diagram of electrospinning.

TABLE 1 | Specimens for the experiment.

Number	EVOH (g)	Silver nitrate solids (g)	Activated carbon powder (g)
1	0.75	0.20	0.15
2			0.55
3			0.85
4		0.50	0.15
5			0.55
6			0.85
7		0.80	0.15
8			0.55
9			0.85
10	1.00	0.20	0.15
11			0.55
12			0.85
13		0.50	0.15
14			0.55
15			0.85
16		0.80	0.15
17			0.55
18			0.85
19	1.25	0.20	0.15
20			0.55
21			0.85
22		0.50	0.15
23			0.55
24			0.85
25		0.80	0.15
26			0.55
27			0.85

2021). Electrospinning is a fiber production technology by stretching charged droplets/jets in an electrostatic field. **Figure 1** illustrates a schematic diagram of the electrospinning process. A precursor solution is stored in the syringe which is connected to the positive pole of the power supply. The positively charged droplet/jet ejected from the syringe is stretched into fine fibers by the force of the electrostatic field during the dynamic "flight" toward the negative pole. The flight also allows for evaporation, and fibers of micron- or nano-level diameters are collected by a low-potential roller or plate and accumulated into nanofiber membranes.

A number of studies on particles filtered using electrospun fibers have been reported recently. Dai et al. (2021) prepared polyacrylonitrile/graphene oxide/polyimide (PAN/GO/PI) composite nanofiber membranes by the electrospinning technology, which demonstrates a filtration efficiency of 99.5% on PM2.5. Activated carbon fiber (ACF) prepared with activated carbon (AC) as the solute has also been used in the field of filtration due to its large specific surface area and large adsorption capacity (Chang et al., 2018). Katepalli et al. (2011) proposed a method for fabricating polyacrylonitrile (PAN) nanofibers with activated carbon microfibers (ACF). The obtained ACF-PANS hierarchical fabrics can effectively control common air pollutants. Nallathambi et al. (2020) investigated a hybrid air filter composite membrane involving soy protein isolate, activated carbon, and polyvinyl alcohol, which can effectively filter not only particulate matter but also toxic gases such as formaldehyde.

Although these composite membranes can effectively filter out submicron particles, they have not been reported to have antibacterial effects. A good environment for microorganism survival is actually provided due to the rich microporosity and a huge specific surface area of carbon fiber membranes (Sakamoto et al., 2020). Therefore, developing a new filter system with a good antibacterial function is much needed. Among inorganic metal antibacterial materials, silver nanoparticles (AgNPs) have become a research focus due to the advantages of a wide antibacterial range, the long effective period of continuous sterilization, and non-drug resistance (Carlos et al., 2020). Zhao et al. (2022) demonstrated that the addition of AgNPs can significantly improve the bacteriostatic rate of stereo-complexed polylactide (sc-PLA) fibers against *Escherichia coli* and *Staphylococcus aureus*. However, the mechanism of the antibacterial properties of AgNPs is not very clear yet. Pallavicini et al. (2018) proposed that the direct nanomechanical action of the high-energy AgNP surface and the slow and sustained release of Ag^+ cations promote the destruction of the bacterial membrane and lead to cell deaths. Yan et al. (2021) verified that both AgNPs and Ag^+ can cause mitochondrial specific toxicity, but the toxicity of AgNP may also come from dissolved Ag^+, which causes exhaustion of reserve respiration and cell deaths by interacting with mitochondria. Baldino et al. (2019) verified that Ag^+ released from PVA films destroys the outer membrane of bacteria mainly by direct contact to achieve the antibacterial effect.

At present, the main synthetic approaches to metal nanoparticles (Ag, Co., Ni, Cu, etc.) include the polysaccharide method, the Tollens reagent method, and radiation and biological methods (Ye et al., 2017; Brycki et al., 2021). Different silver particle reduction methods have also been used in the study of electrospinning to prepare silver-loaded fiber membranes. Emam et al. (2019) successfully synthesized nanoscale spherical AgNPs, AuNPs and PdNPs using alkali-activated dextran whose catalytic performance were also evaluated. Irfan et al. (2021) used the reduction properties of PVP to synthesize silver nanoparticles and prepared PVDF/PVP/AgNP composite membranes with

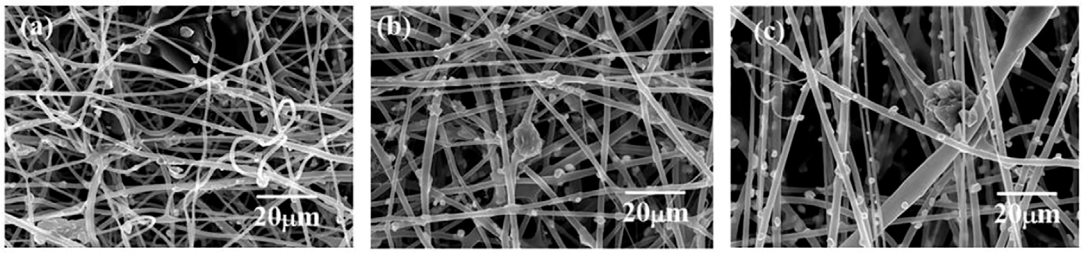

FIGURE 2 | SEM of AgNP-AC composite fiber membrane with silver concentration of 0.05 g/ml, activated carbon concentration of 0.055 g/ml, and EVOH of **(A)** 7.5%, **(B)** 10.0%, and **(C)** 12.5%.

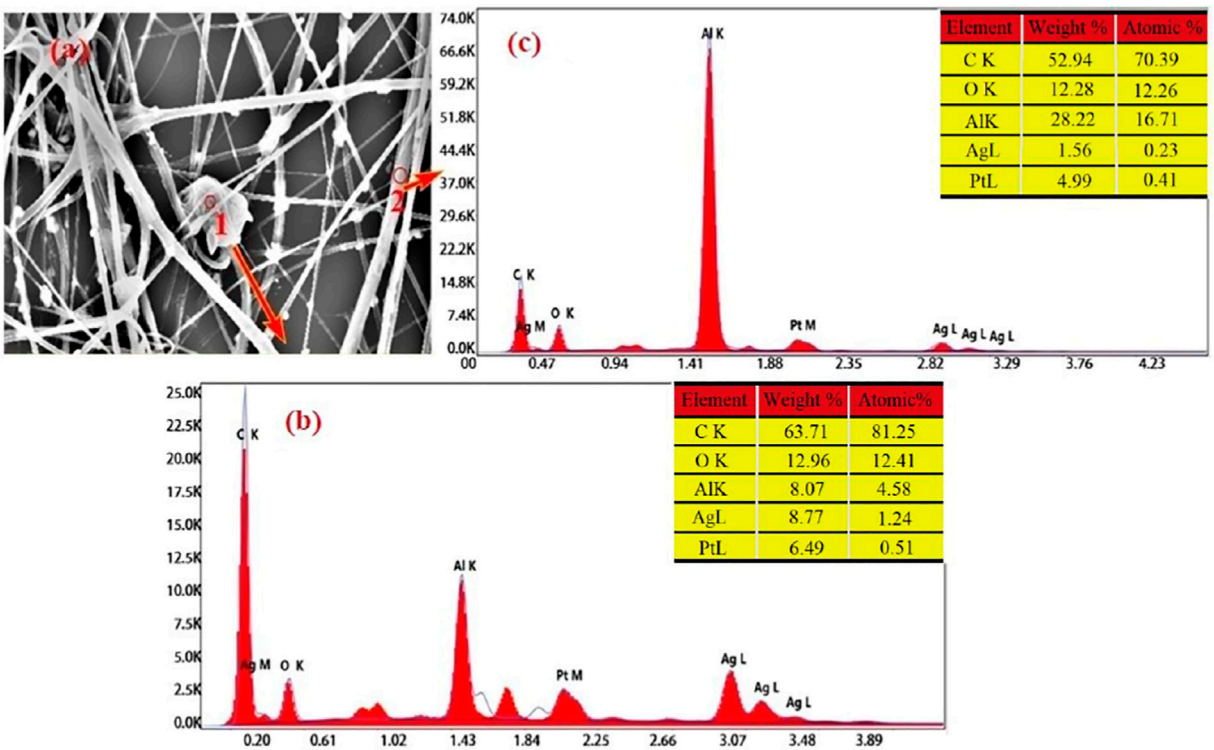

FIGURE 3 | Information of AgNP-AC composite fiber membrane with 7.5% of EVOH, 0.03 g/ml of Ag, and 0.02 g/ml of AC **(A)** SEM, **(B)** EDX of part 1, and **(C)** EDX of part 2.

antibacterial properties by electrospinning. Sandri et al. (2019) fabricated an electrospun scaffold loaded with silver nanoparticles (AgNPs) with the colloidal suspension of AgNPs by using $NaBH_4$ as a reducing agent in an acid solution. Emam et al. (2019) fabricated Ag-Au nanocomposites by seed-mediated growth technique with gum arabic and verified their excellent antibacterial properties. The photocatalytic reaction was also shown to reduce the silver ions in the cellulose skeleton to silver particles (Xu et al., 2011; Ko et al., 2021).

This study proposes a method of compounding silver nanoparticles (AgNPs) with activated carbon using the electrospinning technology, aiming to add a strong antibacterial capacity to filters, which can also absorb heavy metallic ions. The high porosity of activated carbon also provides a good carrying mechanism for AgNPs to minimize aggregation of nanoparticles, resulting in a more evenly dispersed AgNPs on fibers and better antibacterial activity and efficiency (Álvarez et al., 2021; Nicosia et al., 2016). The precursor solution was prepared with an isopropanol solution containing polyethylene-vinyl alcohol (EVOH), silver nitrate, and powdered activated carbon. The surface morphology and fiber diameter of the composite fiber was characterized and analyzed by scanning electron microscope (SEM) and energy-dispersive X-ray spectrometer (EDX). The adsorption and antibacterial properties of fabricated composite fiber membranes were evaluated.

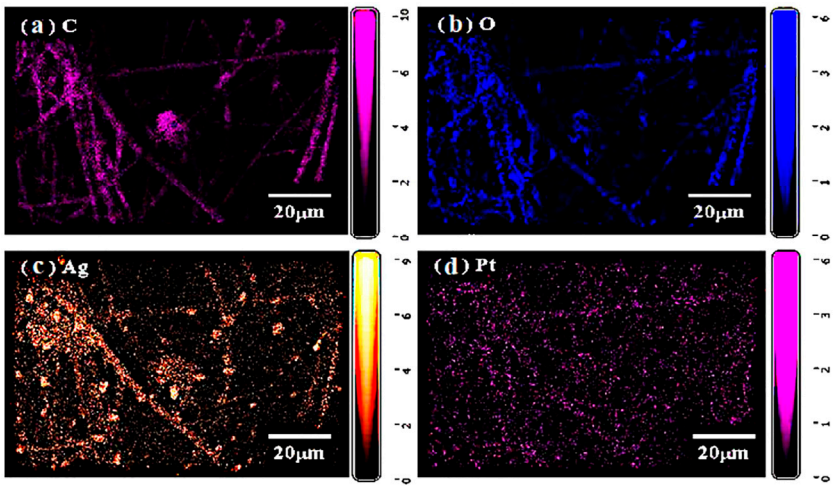

FIGURE 4 | Elemental mapping of partial AgNP-AC composite fibers **(A)** carbon, **(B)** oxygen, **(C)** silver, and **(D)** platinum.

MEMBRANE FABRICATION AND CHARACTERIZATION

Agents and Devices

The materials used in producing the filtering membranes include isopropanol (C_3H_8O, 99.5%, from Shaanxi Huaxing Experiment Technology Co., Ltd.), powdered activated carbon (AC), silver nitrate solid ($AgNO_3$), polyvinyl alcohol (EVOH, from Sigma-Aldrich. Batch number: 12822PE).

A commercial electrospinning device was used to fabricate fiber membranes. A scanning electron microscope (SEM), energy-dispersive X-ray spectrometer (EDX), and an inductively coupled plasma emission spectrometer were used to characterize the fibers' physical and chemical features.

Preparation of Precursor Solution of AgNP-AC Composite Nanofiber Membranes.

A solution mixed with 7 ml isopropanol and 3 ml deionized water was used as the solvent. EVOH particles of 1.25, 1.0, and 0.75 g were added to the solution to obtain three different concentrations, respectively; the solutions were heated at 75°C by a magnetic stirrer, while silver nitrate solids (0.20, 0.50, and 0.80 g) were added, followed by addition of activated carbon powders (0.15, 0.55, and 0.85 g). In total, 27 compositions are used as shown in **Table 1**.

Fabrication of AgNP-AC Composite Nanofiber Membranes

The principle and layout of the electrospinning process are indicated in **Figure 2**. A voltage of 18 KV was provided between the syringe injector and the fiber collector. The standoff distance from the syringe needle to the collector was 15 cm, and the rotation speed of the receiving roller was kept at 500 r/min. The injection speed (the speed of plunger movement) was set at 0.0063–0.0126 ml/min for different fiber diameters. Meanwhile, the environmental temperature was kept between 40 and 45°C to avoid needle blockage by crystallization of the solution. An AgNP-AC composite nanofiber membrane was formed on the roller following electrospinning over a certain time and was finally removed for assessment and tests after irradiation by a UV lamp (20–40 W) installed in the device.

Morphology and Material Characterization

A scanning electron microscope (SEM) was used to observe the morphology and silver nanoparticles and activated carbon particles on the surface of AgNP-AC composite nanofibers. Energy-dispersive X-ray spectroscopy (EDX) was also applied to observe the constituent elements of the particles on the fiber surface.

In aerosols that make up haze, the most harmful substances are industrial pollution, including airborne heavy metal particles and organic matters. Activated carbon is proven to be effective for the adsorption of heavy metal ions due to its specific microporous/ultra-microporous structure (Zaini et al., 2021). Cu(II) is a highly toxic pollutant harmful to humans, which is often seen being discharged by the metallurgy, printing, fertilizer, and other industries (Yu et al., 2021). Therefore, it is of interest to assess the effectiveness of AgNP-AC composite nanofiber membranes for Cu(II) adsorption.

Yan et al. (2018) found that a higher temperature is beneficial in promoting the adsorption capacity of the composite fibers with larger nanosilver particles easily activated. While a low pH value of the solution reduces the adsorption capacity of the fiber. This is due to the protonation reaction of functional groups such as the amino and carboxyl groups on the fiber surface with a strong acid condition. Also the competition between heavy metal ions and H^+ is intensified, which affects the fixation of heavy metal ions onto the fiber membranes (Min

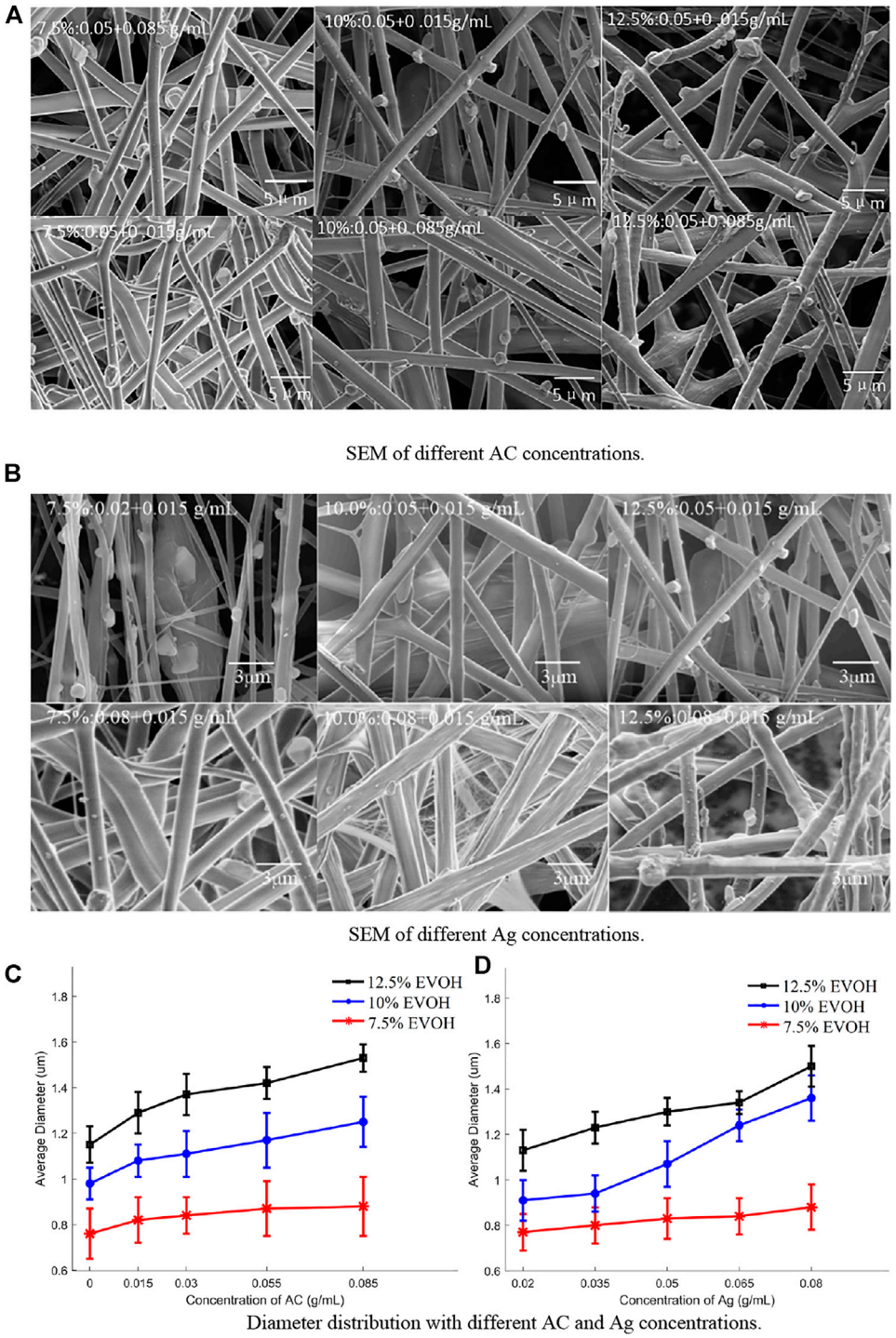

FIGURE 5 | (A) SEM of different AC concentrations. **(B)** SEM of different Ag concentrations. **(C, D)** Diameter distribution with different AC and Ag concentrations.

et al., 2012; Martín et al., 2018). Based on these, the copper solution of 1000 mg/L concentration was diluted with deionized water to 110 mg/L, 90 mg/L, 60 mg/L, and 25 mg/L, respectively, then adjusted to pH 8 with 0.1 mol/L HCl or 25% $NH_3{\cdot}H_2O$ solution. The membranes of AgNP-AC composite were put into the diluted solutions containing copper ions in a water bath oscillator and kept at 45°C for 240 min. The concentrations of copper ions in the solution were then measured by an inductively coupled plasma emission spectrometer (ICP-OES).

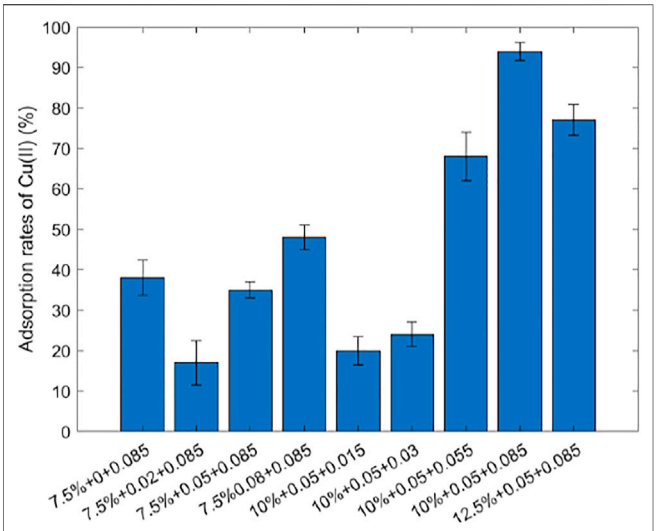

FIGURE 6 | AgNP-AC composite fibers membrane for Cu(II) adsorption rate distribution.

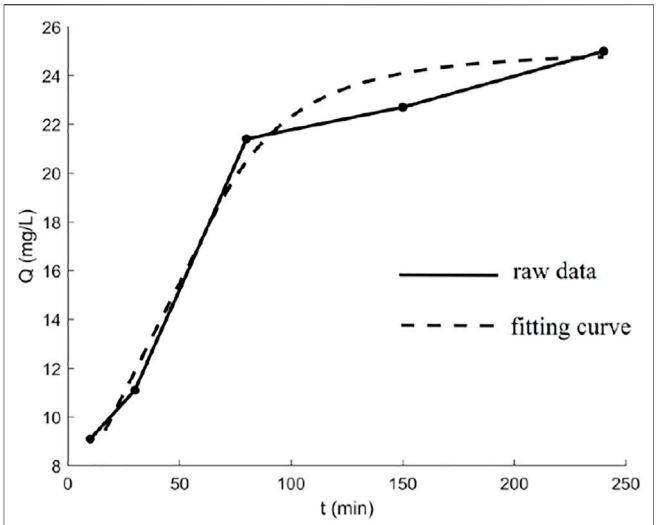

FIGURE 8 | Contact time of Cu(II) the influence of adsorption.

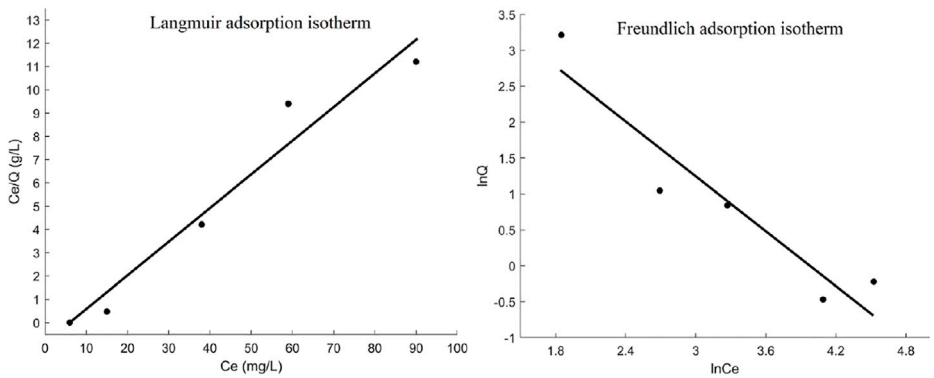

FIGURE 7 | Cu(II) adsorption isotherm models of the fitting.

The antibacterial performance of the membrane was evaluated by the bacteriostatic ring test using *Staphylococcus aureus* (Ryšánek et al., 2019; Wang et al., 2018). Resuscitated bacteria liquid was divided into three tubes, each containing 3 ml of culture medium. The tubes were then kept overnight in a water bath in a shaker at 37°C. The bacterial liquid was then put into a petri dish (20 ml/dish) and kept sealed at 4°C after cooling, ready for use. For the ring test, 0.5 ml of bacterial liquid was spread onto the petri dish evenly with an inoculation loop or a sterile pipette tip. Four circular cuts of fiber membranes with different AgNP or activated carbon concentrations were placed with distance into a dish, which was then kept in an incubator at 37°C for 4, 8, 12, 24, 36, and 48 h, respectively, diameters of bacteriostatic circles in the dish were then measured as the quantitative assessment of the inhibitory effect.

RESULTS AND DISCUSSIONS

Fiber Morphology Analysis

SEM images of fibers corresponding to different concentrations of EVOH (7.5, 10.0, 12.5%) are shown in **Figures 2A–C**. It can be seen in the 3D microstructure network of the random and disorienting arrangement of fibers. The diameter distribution of the AgNP-AC composite fiber was measured in the range of 750–1900 nm. Also, there are a large number of AgNPs on the surface and inside of the composite fibers.

Figure 3 1) SEM image of the composite fiber with an EVOH concentration of 7.5%, a silver concentration of 0.03 g/ml, and an activated carbon concentration of 0.02 g/ml. The surface of the fiber characterized by energy spectrum and the EDX diagram of the elements contained in the composite fiber are shown in **Figures 3B,C**. It can be found that the composite fibers

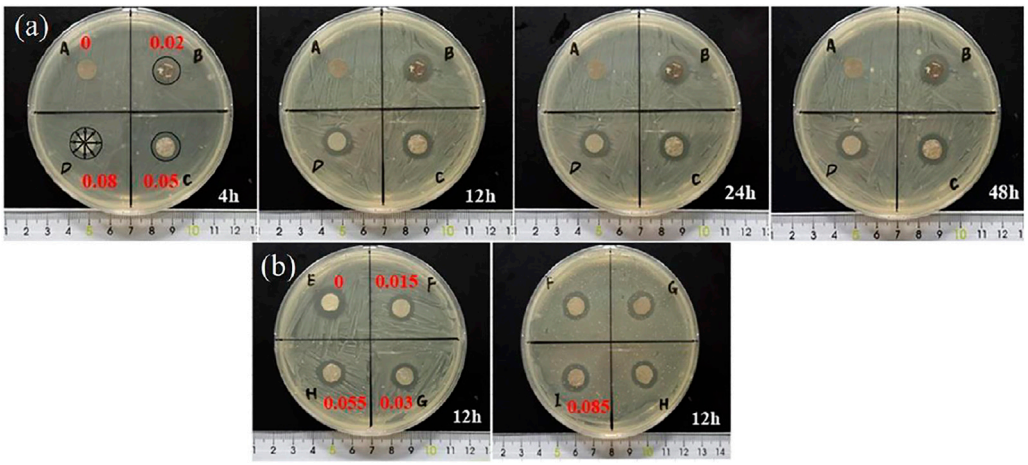

FIGURE 9 | Zones of inhibition against *S. aureus* bacteria by AgNP-AC composite fiber membranes of different time; **(A)** corresponding to different silver concentrations: 0, 0.02 g/ml, 0.05 g/ml, and 0.08 g/ml; **(B)** corresponding to different activated carbon concentrations: 0, 0.015 g/ml, 0.03 g/ml, 0.055 g/ml, and 0.085 g/ml.

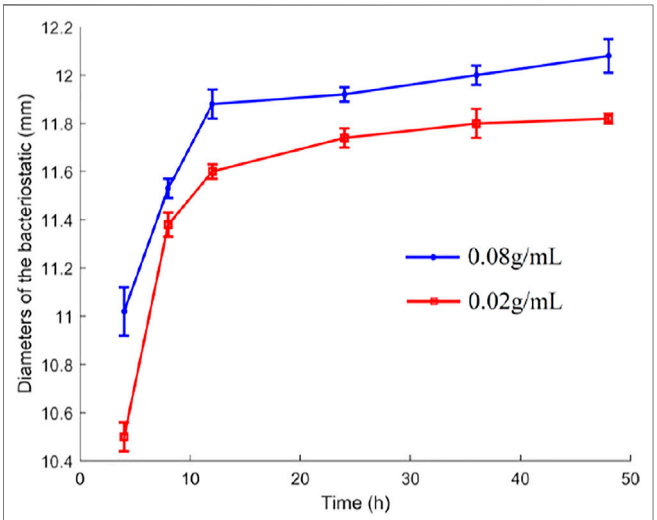

FIGURE 10 | Effect of silver concentration on diameters of the inhibition ring.

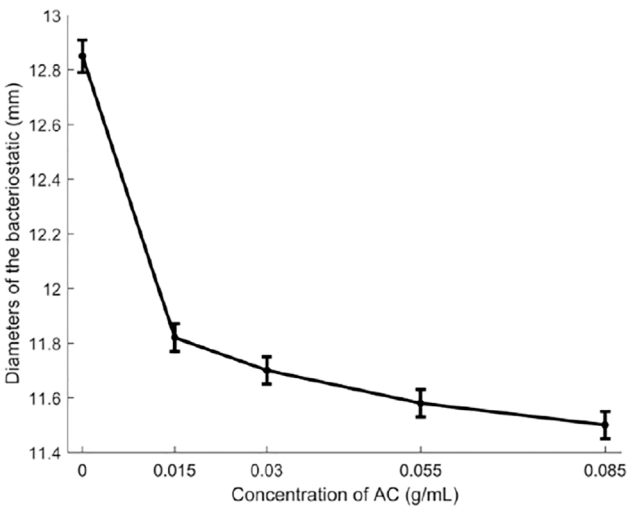

FIGURE 11 | Effect of activated carbon concentration on the diameters of inhibition ring.

contain four main elements: C, O, Ag, and Pt, while the high Al from the aluminum foil is used to collect the fibers. Among them, Pt was attached to the fiber surface due to the gold sputter coaters for observation. **Figures 4A–D** are element mapping diagrams of AgNP-AC composite fiber, which verifies the distribution of elements in the composite fiber. Among the four elements contained in the fiber, the carbon element has the largest proportion at 63.71% (wt%). A part of the carbon elements is distributed as a block structure, while most are evenly distributed on the surface of the composite fibers. The silver particles on the fiber surface indicate that the connection with activated carbon may be reliable (Duan et al., 2018).

Process Parameter Analysis

Diameters of nanofibers were measured using ImageJ (Collins, 2007) software to analyze the influence of different material concentrations on the fiber diameter. **Figures 5A,B** show SEM images of the composite fibers with different concentrations of silver and activated carbon with the same EVOH concentration.

As shown in **Figure 5C**, the diameter of the composite fiber increases as the concentration of activated carbon increases. This is because of the increased adhesion on the surface of the droplets/jet, resulting from the addition of activated carbon to the spinning solution. The degree of stretching is thus gradually weakened, resulting in increases in fiber diameters with the same electric field force.

Figure 5D shows the influence of the silver concentration on the average diameter of fibers. As the silver concentration increases, fiber diameters increase. Due to the electrical conductivity of silver, the electric field is weakened with less spinning forces, resulting in larger fiber diameters.

It can also be seen from both **Figures 5C,D** that a higher concentration of EVOH leads to larger fiber diameters. EVOH increases the viscosity of the solution, reducing the stretching effect of the electric field force during the fiber formation, thus yielding in larger fiber diameters. This has also been verified in previous work (Zhang, et al., 2018).

From these figures, the size of silver particles was also estimated and is found to be in the range of about 0.1 μm (100 nm) to 1.5 μm, with the average being close to 1 μm. A more detailed measurement of the silver particle size and its effect on the antibacterial function will be conducted in future works.

Adsorption Performance Test

The adsorption rates of Cu(II) by tested AgNP-AC composite nanofiber membranes are shown in **Figure 6**. As can be seen, the best adsorption performance, with an adsorption rate of 94.07% for Cu(II), is achieved by membranes made from 10% EVOH, 0.05 g/ml silver nanoparticle, and 0.085 g/ml activated carbon concentration. The adsorption pattern of this composite fiber membrane can be obtained by the curve fitting of Langmuir and Freundlich isotherm models in **Eqs 1**, **2** (Nnadozie and Ajibade, 2020; Dandil et al., 2019) using the experimental data, as shown in **Figure 7**.

$$\frac{C_e}{q_e} = \frac{C_e}{Q_m} + \frac{1}{k_L Q_m} \tag{1}$$

$$ln\, q_e = ln\, k_F + \frac{1}{n} ln\, C_e \tag{2}$$

where Q_m is the maximum adsorption capacity, k_L the Langmuir equilibrium constant, k_F the Freundlich equilibrium constant, **n** is the constant related to the adsorption capacity, and C_e is the equilibrium concentration.

Figure 7 shows the two isotherm model fitting diagrams of Langmuir (R^2 = 0.9573) and Freundlich (R^2 = 0.8912), respectively, With a higher coefficient of determination (R^2), the Langmuir model appears to be the better one to describe the adsorption of Cu(II) by AgNP-AC composite fiber membranes. As reported by Ghosal and Gupta (2017), following the Langmuir model means a more uniform distribution. In addition, the balance parameter R_L, also called the separation factor as a dimensionless constant, can express the basic characteristics of Langmuir isotherms. The value of R_L can be calculated by **Eq. 3** (Stromer et al., 2018).

$$R_L = 1/(1 + K_L C_0) \tag{3}$$

where C_0 (mg/L) is the initial concentration of heavy metal ions in the solution. Thus, the value of the equilibrium parameter R_L (irreversible: R_L = 0, favorable: 0< R_L <1, linear: R_L = 1, unfavorable: R_L >1) in the Langmuir model was calculated as 0.05 for this test, which indicates that the adsorption is developing in a favorable direction.

Figure 8 illustrates the influence of the contact time on adsorption. As the contact time increases, the adsorption of Cu(II) by the composite fiber membranes increases. The adsorption shows a higher rate in early time. After fitting the raw data, the adsorption equilibrium time can be regarded as approximately 240 min with the absorption rate reaching a plateau value.

Antibacterial Properties of AgNP-AC Composite Nanofiber Membranes

The antibacterial experiment results of fiber membranes at different times are shown in **Figure 9** for different AgNPs or activated carbon concentrations. Diameters of bacteriostatic circles in the dish were measured as an indicator of the inhibitory effect. It can be observed from **Figure 9** that various bacteriostatic rings were formed around the circular patches of membrane containing silver nanoparticles, while there was no such ring around the composite nanofiber patch without silver nanoparticles.

Figures 10, **11** show the influence of different concentrations of silver and activated carbon on the measured diameters of antibacterial rings against the incubation time. It can be seen from **Figure 10** that ring diameters increase with the silver concentration. And the rate of increase was fast in the early hours, and then slowed down with time, which is similar to the results of other studies (Ahmed et al., 2019; Mostafa et al., 2022).

In contrast, as the concentration of the activated carbon increases, the diameters of the bacteriostatic ring gradually decrease as shown in **Figure 11**. As the content of activated carbon increases, more adsorption sites exist which cause part of the silver particles are embedded in the fiber. Therefore, the number of silver particles exposed on the surface of the fiber is reduced which ultimately affects the antibacterial capacity.

CONCLUSION

In this study, a fabrication method to prepare AgNP-AC composite fiber membranes by electrospinning was proposed. The structural characteristics, adsorption, and antibacterial properties of the fiber membranes obtained were analyzed. The following conclusions can be drawn:

1) Morphology and structure of the electrospun membranes observed by SEM and EDX show that the surface of the AgNP-AC composite fibers is not smooth due to a large number of silver particles and activated carbon particles, which are uniformly distributed on the fiber surface.
2) AgNP-AC composite fiber membranes made from the solution containing 10% EVOH, 0.05 g/ml Ag, and 0.085 g/ml activated carbon show the best performance of adsorption of Cu(II) at 94.07%.
3) Adsorption performance of Cu(II) can be suitably described by the Langmuir model.

4) Antibacterial performance of AgNP-AC composite fiber membranes is enhanced by the silver particles, with the effect particularly strong in the early hours.
5) Antibacterial performance of AgNP-AC composite fiber membranes can be inhibited by activated carbon, particularly at a higher content of the latter.

The adsorption and antibacterial properties of composite nanomaterials were tested and verified in this study. The raw materials used to manufacture AgNP-AC composite fiber membranes are economical, environmentally friendly, widely, and sustainably available. With its good adsorption and antibacterial performance, the fiber membranes show strong potential in filtration uses in domestic, industrial, and clinical applications.

DATA AVAILABILITY STATEMENT

The original contributions presented in the study are included in the article/Supplementary Material, further inquiries can be directed to the corresponding authors.

AUTHOR CONTRIBUTIONS

WQ: investigation and data curation. CX: conceptualization, methodology, investigation, and validation. DL: draft preparation and validation. BW: conceptualization, methodology, and review and editing, and CZ: funding acquisition.

FUNDING

This research was funded under the project "Innovative Talent Promotion Plan—Science and Technology Innovation Team" (funding ID 2021TD-27) by Shaanxi Provincial Department of Science and Technology.

ACKNOWLEDGMENTS

The authors would also like to acknowledge the funding support received for this research. We would also like to acknowledge the reviewers for providing comments and advice which have help to enhance the quality of this study.

REFERENCES

Ahmed, H. B., Attia, M. A., El-Dars, F. M. S. E., and Emam, H. E. (2019). Hydroxyethyl Cellulose for Spontaneous Synthesis of Antipathogenic Nanostructures: (Ag & Au) Nanoparticles versus Ag-Au Nano-alloy. *Int. J. Biol. Macromolecules* 128, 214–229. doi:10.1016/j.ijbiomac.2019.01.093

Álvarez, M. L., Méndez, A., Rodríguez-Pacheco, R., Paz-Ferreiro, J., and Gascó, G. (2021). Recovery of Zinc and Copper from Mine Tailings by Acid Leaching Solutions Combined with Carbon-Based Materials. *Appl. Sci.* 11, 5166–5211. doi:10.3390/app11115166

Baldino, L., Aragón, J., Mendoza, G., Irusta, S., Cardea, S., and Reverchon, E. (2019). Production, Characterization and Testing of Antibacterial PVA Membranes Loaded with HA-Ag3 PO4 Nanoparticles, Produced by SC-CO2 Phase Inversion. *J. Chem. Technol. Biotechnol.* 94, 98–108. doi:10.1002/jctb.5749

Brycki, B., Szulc, A., and Babkova, M. (2021). Synthesis of Silver Nanoparticles with Gemini Surfactants as Efficient Capping and Stabilizing Agents. *Appl. Sci.* 11, 154. doi:10.3390/app11010154

Chang, F.-C., Yen, S.-H., and Wang, S.-H. (2018). Developing Lignosulfonate-Based Activated Carbon Fibers. *Materials* 11, 1877. doi:10.3390/ma11101877

Chen, K.-N., Sari, F. N. I., and Ting, J.-M. (2019). Multifunctional TiO2/polyacrylonitrile Nanofibers for High Efficiency PM2.5 Capture, UV Filter, and Anti-bacteria Activity. *Appl. Surf. Sci.* 493, 157–164. doi:10.1016/j.apsusc.2019.07.020

Collins, T. J. (2007). ImageJ for Microscopy. *Biotechniques* 43, S25–S30. doi:10.2144/000112517

Dai, H., Liu, X., Zhang, C., Ma, K., and Zhang, Y. (2021). Electrospinning Polyacrylonitrile/Graphene Oxide/Polyimide Nanofibrous Membranes for High-Efficiency PM2.5 Filtration. *Separat. Purif. Tech.* 276, 119243. doi:10.1016/j.seppur.2021.119243

Dandil, S., Akin Sahbaz, D., and Acikgoz, C. (2019). Adsorption of Cu(II) Ions onto Crosslinked chitosan/Waste Active Sludge Char (WASC) Beads: Kinetic, Equilibrium, and Thermodynamic Study. *Int. J. Biol. Macromolecules* 136, 668–675. doi:10.1016/j.ijbiomac.2019.06.063

Duan, G., Fang, H., Huang, C., Jiang, S., and Hou, H. (2018). Microstructures and Mechanical Properties of Aligned Electrospun Carbon Nanofibers from Binary Composites of Polyacrylonitrile and Polyamic Acid. *J. Mater. Sci.* 53, 15096–15106. doi:10.1007/s10853-018-2700-y

Emam, H. E. (2019). Arabic Gum as Bio-Synthesizer for Ag-Au Bimetallic Nanocomposite Using Seed-Mediated Growth Technique and its Biological Efficacy. *J. Polym. Environ.* 27, 210–223. doi:10.1007/s10924-018-1331-3

Emam, H. E., Mikhail, M. M., El-Sherbiny, S., Nagy, K. S., and Ahmed, H. B. (2019). Metal-dependent Nano-Catalysis in Reduction of Aromatic Pollutants. *Environ. Sci. Pollut. Res.* 27, 6459–6475. doi:10.1007/s11356-019-07315-z

Gao, X., Li, Z.-K., Xue, J., Qian, Y., Zhang, L.-Z., Caro, J., et al. (2019). Titanium Carbide Ti3C2Tx (MXene) Enhanced PAN Nanofiber Membrane for Air Purification. *J. Membr. Sci.* 586, 162–169. doi:10.1016/j.memsci.2019.05.058

Ghosal, P. S., and Gupta, A. K. (2017). Determination of Thermodynamic Parameters from Langmuir Isotherm Constant-Revisited. *J. Mol. Liquids* 225, 137–146. doi:10.1016/j.molliq.2016.11.058

Irfan, M., Uddin, Z., Ahmad, F., Rasheed, A., Qadir, M. B., Ahmad, S., et al. (2021). Ecofriendly Development of Electrospun Antibacterial Membranes Loaded with Silver Nanoparticles. *J. Ind. Textiles*, 152808372110125. doi:10.1177/15280837211012590

Juan Carlos, F.-A., Rene, G.-C., Germán, V.-S., and Laura Susana, A.-T. (2020). Antimicrobial Poly (Methyl Methacrylate) with Silver Nanoparticles for Dentistry: A Systematic Review. *Appl. Sci.* 10, 4007. doi:10.3390/app10114007

Katepalli, H., Bikshapathi, M., Sharma, C. S., Verma, N., and Sharma, A. (2011). Synthesis of Hierarchical Fabrics by Electrospinning of PAN Nanofibers on Activated Carbon Microfibers for Environmental Remediation Applications. *Chem. Eng. J.* 171, 1194–1200. doi:10.1016/j.cej.2011.05.025

Khandaker, M., Progri, H., Arasu, D. T., Nikfarjam, S., and Shamim, N. (2021). Use of Polycaprolactone Electrospun Nanofiber Mesh in a Face Mask. *Materials* 14, 4272. doi:10.3390/ma14154272

Ko, S. W., Lee, J. Y., Rezk, A. I., Park, C. H., and Kim, C. S. (2021). *In-situ* Cellulose-Framework Templates Mediated Monodispersed Silver Nanoparticles via Facile UV-Light Photocatalytic Activity for Anti-microbial Functionalization. *Carbohydr. Polym.* 269, 118255. doi:10.1016/j.carbpol.2021.118255

Liu, J., Jiang, T., Li, X., and Wang, Z. L. (2019). Triboelectric Filtering for Air Purification. *Nanotechnology* 30, 292001. doi:10.1088/1361-6528/ab0e34

Martín, D., Faccini, M., García, M. A., and Amantia, D. (2018). Highly Efficient Removal of Heavy Metal Ions from Polluted Water Using Ion-Selective Polyacrylonitrile Nanofibers. *J. Environ. Chem. Eng.* 6, 236–245. doi:10.1016/j.jece.2017.11.073

Matulevicius, J., Kliucininkas, L., Prasauskas, T., Buivydiene, D., and Martuzevicius, D. (2016). The Comparative Study of Aerosol Filtration by Electrospun Polyamide, Polyvinyl Acetate, Polyacrylonitrile and Cellulose

Acetate Nanofiber media. *J. Aerosol Sci.* 92, 27–37. doi:10.1016/j.jaerosci.2015.10.006

Min, M., Shen, L., Hong, G., Zhu, M., Zhang, Y., Wang, X., et al. (2012). Micro-nano Structure Poly(ether Sulfones)/poly(ethyleneimine) Nanofibrous Affinity Membranes for Adsorption of Anionic Dyes and Heavy Metal Ions in Aqueous Solution. *Chem. Eng. J.* 197, 88–100. doi:10.1016/j.cej.2012.05.021

Mostafa, M., Kandile, N. G., Mahmoud, M. K., and Ibrahim, H. M. (2022). Synthesis and Characterization of Polystyrene with Embedded Silver Nanoparticle Nanofibers to Utilize as Antibacterial and Wound Healing Biomaterial. *Heliyon* 8, e08772. doi:10.1016/j.heliyon.2022.e08772

Nallathambi, G., Robert, B., Esmeralda, S. P., Kumaravel, J., and Parthiban, V. (2020). Development of SPI/AC/PVA Nano-Composite for Air-Filtration and Purification. *Rjta* 24, 72–83. doi:10.1108/RJTA-09-2019-0044

Nicosia, A., Keppler, T., Müller, F. A., Vazquez, B., Ravegnani, F., Monticelli, P., et al. (2016). Cellulose Acetate Nanofiber Electrospun on Nylon Substrate as Novel Composite Matrix for Efficient, Heat-Resistant, Air Filters. *Chem. Eng. Sci.* 153, 284–294. doi:10.1016/j.ces.2016.07.017

Nnadozie, E. C., and Ajibade, P. A. (2020). Data for Experimental and Calculated Values of the Adsorption of Pb(II) and Cr(VI) on APTES Functionalized Magnetite Biochar Using Langmuir, Freundlich and Temkin Equations. *Data in Brief* 32, 106292. doi:10.1016/j.dib.2020.106292

Pallavicini, P., Dacarro, G., and Taglietti, A. (2018). Self-Assembled Monolayers of Silver Nanoparticles: From Intrinsic to Switchable Inorganic Antibacterial Surfaces. *Eur. J. Inorg. Chem.* 2018, 4846–4855. doi:10.1002/ejic.201800709

Qiu, H., Tian, L., Ho, K.-f., Pun, V. C., Wang, X., and Yu, I. T. S. (2015). Air Pollution and Mortality: Effect Modification by Personal Characteristics and Specific Cause of Death in a Case-Only Study. *Environ. Pollut.* 199, 192–197. doi:10.1016/j.envpol.2015.02.002

Ryšánek, P., Čapková, P., Štojdl, J., Trögl, J., Benada, O., Kormunda, M., et al. (2019). Stability of Antibacterial Modification of Nanofibrous PA6/DTAB Membrane during Air Filtration. *Mater. Sci. Eng. C* 96, 807–813. doi:10.1016/j.msec.2018.11.065

Sakamoto, H., Fujiwara, I., Takamura, E., and Suye, S.-i. (2020). Nanofiber-guided Orientation of Electrospun Carbon Nanotubes and Fabrication of Aligned CNT Electrodes for Biodevice Applications. *Mater. Chem. Phys.* 245, 122745. doi:10.1016/j.matchemphys.2020.122745

Sandri, G., Miele, D., Faccendini, A., Bonferoni, M. C., Rossi, S., Grisoli, P., et al. (2019). Chitosan/Glycosaminoglycan Scaffolds: The Role of Silver Nanoparticles to Control Microbial Infections in Wound Healing. *Polymers* 11, 1207. doi:10.3390/polym11071207

Stromer, B. S., Woodbury, B., and Williams, C. F. (2018). Tylosin Sorption to Diatomaceous Earth Described by Langmuir Isotherm and Freundlich Isotherm Models. *Chemosphere* 193, 912–920. doi:10.1016/j.chemosphere.2017.11.083

Tian, H., Fu, X., Zheng, M., Wang, Y., Li, Y., Xiang, A., et al. (2018). Natural Polypeptides Treat Pollution Complex: Moisture-Resistant Multi-Functional Protein Nanofabrics for Sustainable Air Filtration. *Nano Res.* 11, 4265–4277. doi:10.1007/s12274-018-2013-0

Wang, Z., Yan, F., Pei, H., Li, J., Cui, Z., and He, B. (2018). Antibacterial and Environmentally Friendly Chitosan/polyvinyl Alcohol Blend Membranes for Air Filtration. *Carbohydr. Polym.* 198, 241–248. doi:10.1016/j.carbpol.2018.06.090

Xu, C., Xu, F., Wang, B., and Lu, T. (2011). Electrospinning of Poly(ethylene-Co-Vinyl Alcohol) Nanofibres Encapsulated with Ag Nanoparticles for Skin Wound Healing. *J. Nanomater.* 2011, 1–7. doi:10.1155/2011/201834

Yan, N., Tang, B. Z., and Wang, W.-X. (2021). Intracellular Trafficking of Silver Nanoparticles and Silver Ions Determined Their Specific Mitotoxicity to the Zebrafish Cell Line. *Environ. Sci. Nano* 8, 1364–1375. doi:10.1039/D1EN00021G

Yan, X.-F., Fan, X.-R., Wang, Q., and Shen, Y. (2018). Adsorption Performance of Silver-Loaded Activated Carbon Fibers. *Therm. Sci.* 22, 11–16. doi:10.2298/TSCI151202141Y

Ye, W. J., Chen, K. H., Cai, S. L., Chen, L. K., Zhong, T. S., and Wang, X. Y. (2017). Progress in Research on Synthesis and Antibacterial Applications of Silver Nanoparticles. *J. Mater. Eng.* 45, 22–30. doi:10.11868/j.issn.1001-4381.2015.001177

Yu, J., Meng, Z., Yan, S., Zhao, S., Zhu, B., Cai, X., et al. (2021). Precise Control of Ultramicropore Structure of Activated Carbon Fiber for the Application of Cu(II) Adsorption/electro-Adsorption. *J. Environ. Chem. Eng.* 9, 105312. doi:10.1016/j.jece.2021.105312

Zaini, M. A. A., Zhi, L. L., Hui, T. S., Amano, Y., and Machida, M. (2021). Effects of Physical Activation on Pore Textures and Heavy Metals Removal of Fiber-Based Activated Carbons. *Mater. Today Proc.* 39, 917–921. doi:10.1016/j.matpr.2020.03.815

Zhang, C., Liu, D., Xu, C., Liu, D., and Wang, B. (2018). Tensile Properties of Ag-EVOH Electrospinning Nanofiber Mats for Large Muscle Scaffolds. *Mech. Adv. Mater. Structures* 27, 1312–1321. doi:10.1080/15376494.2018.1508794

Zhao, S. Y., Ke, H. Z., Yang, T. T., Peng, Q. Q., Ge, J. L., Yao, L. R., et al. (2022). Enhanced Thermal and Antibacterial Properties of Stereo-Complexed Polylactide Fibers Doped with Nano-Silver. *Front. Mater.* 9, 775333. doi:10.3389/fmats.2022.775333

Conflict of Interest: The authors declare that the research was conducted in the absence of any commercial or financial relationships that could be construed as a potential conflict of interest.

Publisher's Note: All claims expressed in this article are solely those of the authors and do not necessarily represent those of their affiliated organizations, or those of the publisher, the editors, and the reviewers. Any product that may be evaluated in this article, or claim that may be made by its manufacturer, is not guaranteed or endorsed by the publisher.

Copyright © 2022 Liu, Zhang, Wang, Quan and Xu. This is an open-access article distributed under the terms of the Creative Commons Attribution License (CC BY). The use, distribution or reproduction in other forums is permitted, provided the original author(s) and the copyright owner(s) are credited and that the original publication in this journal is cited, in accordance with accepted academic practice. No use, distribution or reproduction is permitted which does not comply with these terms.